Int J Biochem Mol Biol 2011;2(1):67-77
www.ijbmb.org /ISSN:2152-4114/IJBMB1011003

Original Article

Structural analysis of NADPH depleted bovine liver catalase and its inhibitor complexes

Ragumani Sugadev[1,*], M.N.Ponnuswamy[2,*], K. Sekar[3]

[1]Bioinformatics Centre, Defense Institute of Physiology and Allied Science, Lucknow Road, Timarupr, Delhi-110054, India; [2]Department of Crystallography and Biophysics University of Madras, Guindy Campus, Madras - 600 025, India. [3]Bioinformatics Centre, Supercomputer Education and Research Centre, Indian Institute of Science, Bangalore - 560 012, India. [*]Both authors contributed equally to this work.

Received November 29, 2010; accepted January 28, 2011; Epub January 29, 2011; Published February 15, 2011

Abstract: To study the functional role of NADPH during mammalian catalase inhibition, the X-ray crystal structures of NADPH-depleted bovine liver catalase and its inhibitor complexes, cyanide and azide, determined at 2.8Å resolution. From the complex structures it is observed that subunits with and without an inhibitor/catalytic water molecule are linked by N-terminal domain swapping. Comparing mammalian- and fungal- catalases, we speculate that NADPH-depleted mammalian catalases may function as a domain-swapped dimer of dimers, especially during inactivation by inhibitors like cyanide and azide. We further speculate that in mammalian catalases the N-terminal hinge-loop region and α-helix is the structural element that senses NADPH binding. Although the above arguments are speculative and need further verification, as a whole our studies have opened up a new possibility, viz. that mammalian catalase acts as a domain-swapped dimer of dimers, especially during inhibitor binding. To generalize this concept to the formation of the inactive state in mammalian catalases in the absence of tightly bound NADPH molecules needs further exploration. The present study adds one more intriguing fact to the existing mysteries of mammalian catalases.

Keywords: NADPH, bovine liver catalase, domain swapping

Introduction

Although catalases have been studied for more than 100 years, research continues to reveal differences in the functions of mammalian catalases compared to those of prokaryotes. Thus, they display oxidase activity, and use unbound NAD(P)H to prevent substrate inactivation without displacing catalase-bound NADP(+) [1]. Studies on catalase also have gained momentum recently owing to their postulated impact in extending life-span [2-4]. Nearly all aerobic organisms contain catalase, a well-characterized homotetrameric antioxidant enzyme that scavenges the toxic free radical H_2O_2 from cells by decomposing it into water and oxygen. Catalases that interact with NADPH include those of bovine liver (BLC), human erythrocytes (HEC), the Gram-negative facultative anaerobic bacterium *Proteus mirabilis* (PRC), the fungus *Saccharomyces cerevisiae* (SCC-A), and the bacterium *Micrococcus lysodeikticus* (MLC) [5-9]. Based on the number of aminoacids in each monomer the catalases classified into small and large subunit catalases. The small subunit catalases are around 500 amino-acid residues per monomer. The structures of these catalases , together with biochemical studies, demonstrate that NADPH interacts more strongly with mammalian catalases than with fungal- and bacterial-catalases [10]; among these small subunit catalases, BLC particularly has been extensively studied. BLC comprises four subunits, with three non-equivalent interfaces represented by the three axes P, R, and Q axis, following the nomenclature of [5]. **Figure 1** shows the Q-axis related dimers in blue and gray. Each subunit consists of an eight-stranded β-barrel, and α-helical domain at its one face. The swapped Q-axis-related dimers are formed by an N-terminal α-helix (red: residue 3-69) of one subunit that is hooked through/in a wrapping loop (green: residue 379-437) of the other subunit. The NADPH binds to the cleft between

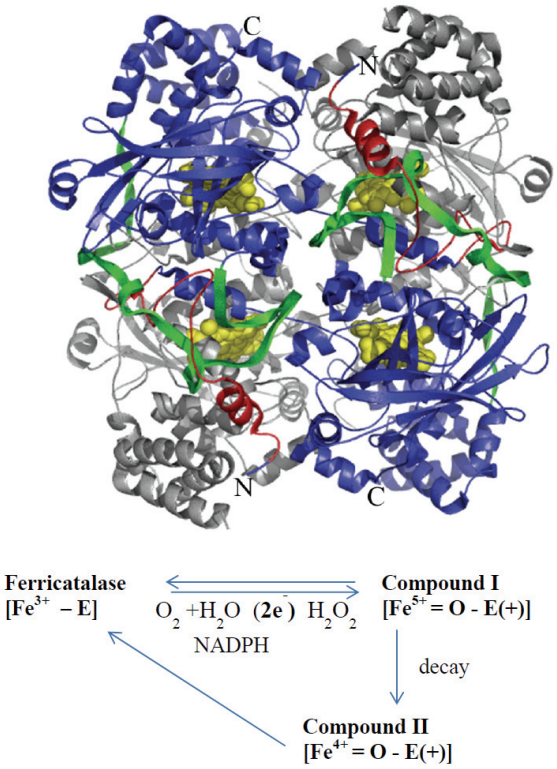

Figure 1. Crystal structure of wild type catalase (BLC without NADPH: PDB ID 1TGU). The heme moieties are shown in yellow color and their atoms are represented as spheres. The N and C-terminals of Q axis related domain swapped dimer (blue color) are labeled. Scheme for NADPH oxidation by catalase and protect the enzyme from inactivation through compound II state formation.

the β-barrel and the α-helical domains [5].

The enzyme cleaves two molecules of hydrogen peroxide into two water molecules and one oxygen molecule in a normal reaction cycle that involves the formation of a compound I state (Fe^{5+}=O) [11-13]. When there is a delay in the steady supply of H_2O_2 an interaction with oxidation substances, such as the superoxide radical ($O2^{-}$), phenols, and ferrocyanide leads to the formation of the compound II state, wherein compound I is reduced by a single electron [14-17]. The compound II state is reduced to the native state either spontaneously, or through the oxidation of NADPH to $NADP^+$ [18].

In BLC, the bound NADPH plays many functions apart from reversing the inactivation state. NADPH lowers the formation of compound II and increases the rate of its removal [10]. The former action predominates over the latter; Kirkman et al.suggested that NADPH might protect catalase from oxidative damage through actions broader than merely preventing the formation of compound II [19]. Observations suggest that NADPH also mediates in the inactivation of BLC by monochloroamine (NH_2Cl) and Dithioerythritol (DTE) [20,21]. The catalase from *Aspergillus niger*, was less sensitive to NH_2Cl than BLC, and was not sensitized by added NADPH [20]. The allosteric effect in bovine liver catalase during irreversible inhibition by effectors was postulated, although the hypothesis still lacks experimental proof [22].

To study the role of NADPH during inactivation, we completely removed NADPH from all the four subunits of BLC, and solved the structure of NADPH-depleted BLC (wild type) with the potent inhibitors, cyanide and azide. Two of the subunits of these structures and their complexes with cyanide and 3-amino1,2,4-triazole were compared to BLC and to HEC with NADPH [6]. Based on the analysis we propose that NADPH-depleted mammalian catalase may function as a domain-swapped dimer of dimers, especially during inactivation by inhibitors like azide and cyanide. We speculated that the N-terminal hinge-loop region and the α-helix is the possible structural element that senses the NADPH binding in mammalian catalase.

Methods

Preparation of BLC without NADPH, and assessments of its activity

Bovine liver catalase (EC 1.11.16; hydrogen peroxide oxidoreductase) was purchased from Sigma Chemicals. We removed NADPH from BLC using the dye-ligand affinity chromatography with Red-A matrix gel containing Procine HE3B [21]. The protein was dialysed in 0.1M Tris-HCl buffer (pH 7.5), loaded on the column, and washed with the same buffer. The bound BLC was eluted by 0.5mM of adenine diphosphate (ADP). In concord with Jouve's result, only 35% of the protein was recovered from the column. The ADP was removed by dialyzing in 0.1M Tris HCl (pH 7.0) overnight at 4°C. Catalase activity was determined polarogaphically in 50mM phosphate buffer at the physiological pH 7.0, using a Clark-type electrode (YSI 5331 Oxygen probe) at 25°C. We also determined cata-

Table 1. Data collection and refinement

	Wild type	Wild type complexed with cyanide	Wild type complexed with azide
Data Set			
Cell dimensions	*a*=85.53 Å *b*=139.67 Å *c*=225.14 Å α=b = γ=90°	*a*=86.06 Å *b*=140.11 Å *c*=226.51 Å α=b=γ=90°	*a*=86.27 Å *b*=140.93 Å *c*=230.69 Å α=b = γ =90°
Space group	$P2_12_12_1$	$P2_12_12_1$	$P2_12_12_1$
Data Collection Statistics			
Wavelength (Å)	1.0062	1.0062	1.0062
Resolution range (Å)	50.0-2.8	50.0-2.8	50.0-2.8
Outermost Shell (Å)	2.80-2.90	2.80-2.90	2.80-2.90
Unique reflections	64055	58589	65743
Completeness (%)	95.1(68.3)	93.1(66.5)	98.0(70.2)
Mean I/σ(I)	14.2	12.7	15.7
Redundancy	13(3.0)	12(2.4)	13(3.2)
R_{merge}[a]	0.114(0.436)	0.123(0.480)	0.095(0.41)
Refinement Statistics			
No. of reflections (work)	60442	52146	61545
No. of reflections (test)	1822	1553	1859
R_{factor}[b]/R_{free}[c]	0.20/0.25	0.20/0.26	0.23/0.28
Resolution range (Å)	40 -2.8	39.2-2.8	39-2.8
R.M.S.D. bond lengths (Å)	0.014	0.018	0.013
R.M.S.D. bond angles (°)	3.0	3.4	3.2
<B-values>	32	31	31
Main-chain (Å^2)	29	29	30
Sidechain (Å^2)	33	32	31
Number of non-H atoms	16068	16068	16068
heteroatoms	172	176	175
water molecules	933	688	806

Values for the highest resolution shell are given within parentheses

[a]$R_{merge} = \Sigma \mid Ii - \langle I \rangle \mid / \Sigma \mid Ii \mid$ where Ii is the intensity of the ith measurement, and <I> is the mean intensity for that reflection.

[b]$R_{factor} = \Sigma \mid\mid F_{obs}\mid - \mid F_{calc}\mid\mid / \Sigma \mid F_{obs}\mid$, where $\mid F_{obs}\mid$ and $\mid F_{calc}\mid$ are the calculated and observe structure factor amplitudes, respectively.

[c]R_{free} = as for R_{factor}, but for 5% of the total reflections chosen at random and omitted from refinement.

lase activity spectro-photometrically as 43.6 $M^{-1}cm^{-1}$, using an extinction coefficient of hydrogen peroxide at 240nm [23, 24]. One unit of catalase is defined as the amount that decomposes 1mol of H_2O_2 per min at a pH of 7.0 at 25°C.

Crystallization of wild-type catalase and preparation of its cyanide and azide complexes

Wild-type catalase was crystallized at 30mg/ml concentration by the hanging drop vapor diffusion method at 20°C. The protein in 0.1M Tris HCl at pH 7.0 was equilibrated against the same buffer. The cyanide complex of NADPH-depleted catalase was prepared via the vapor diffusion of 10μl of 1M hydrogen cyanide in 1M sodium acetate at pH5.0 [6]; diffusion was continued up to 25 minutes to ensure a full color change in the protein crystals. Diffusion was monitored through formation of insoluble silver cyanide on the same cover slip. Azide complexes of wild-type crystals were grown in 0.1M Tris HCl at pH 7.0, containing 3mM or 10mM sodium azide. Crystals obtained in one week were used to collect X-ray data from wild type catalase and its complexes on orthorhombic crystals that were cryogenically frozen in liquid nitrogen after soaking in a mother liquor containing 30% glycerol as a cryoprotectant. The X-ray data was collected at the National Synchrotron Light Source's (NSLS's) beam line X29 us-

ing an ADSC Q-315 CCD detector. The X-ray data were processed with the HKL2000 package software [25].

Structure determination and refinement

Table 1 summarizes the data collected, its reduction, and the structure refinement statistics. The structure of bovine liver catalase without NADPH was determined by the molecular replacement method with AmoRe using 4BLC as the model [26]. This model was built using the O program [27], and refined with CNS [28]. The randomly selected 10% of the data were set aside for the R_{free} calculation. The refinement included the overall anistropic B factor and bulk solvent correction. For model building, we employed the 2Fo-Fc, Fo-Fc and composite omit maps.

Structure analysis

Analysis of the stereo chemical quality of the protein model and assignment of secondary structure were conducted with PROCHECK [29]. Superposition of human catalase with NADPH-depleted catalase was accomplished using the package Insight II. We assessed the accessible surface area of individual residues using the program NACCESS [30]. The figures were prepared with PyMol [31].

Protein Data Bank accession numbers

The 2.8Å-resolution structures of the wild type catalase and its complexes with azide and cyanide were deposited in the Protein Data Bank; their respective accession numbers are 1TGU, 1TH2, and 1TH3.

Results

Overall quality of the structures

Structure analysis of wild type catalase and its azide and cyanide compounds, carried out by PROCHECK [29] and CNS 1.1 [28], showed that the overall stereo chemical statistics are good in all structures (Table 1). This is evident from the final R-factors; viz for wild type catalase (R_{free} =25: R=20), (R_{free} = 28; R= 23) for wild-type azide complex, and (R_{free} =26; R=20) for wild-type cyanide complex. Almost all the residues in them exhibited comparable temperature factors (overall ~31Å^2) except for the N-terminal domain-swapped hinge loop regions (48Å^2). In all the monomers of the hinge-loop region, the residues showed a high temperature factor with an average accessible surface area of 71Å^2. The average accessible surface area (ASA) of each monomer in wild type and complexed structures were 26000Å^2 for the tetramer, the ASA was 61839Å^2. These values are comparable with the findings of [5] for BLC with NADPH. In the wild-type catalase, all four NADPH-binding site pockets showed no electron density for NADPH in the Fo-Fc map and the composite omit map. We made the same observations for the cyanide- and azide-complex structures. These maps also showed that all heme molecules in the active sites of wild type are planar ones.

Crystal packing

The wild-type structure, as well its complexes, contained one tetramer in the asymmetric unit crystallized in the $P2_12_12_1$ space group. The packing of the entire crystal is stabilized along the molecular axes a and b. Only limited molecular interactions stabilize the packing along the c-axis, thereby exposing all four active sites towards the solvent, and consequently, increasing the accessibility of the inhibitor molecule. In human catalase, monomers with NADPH are in different packing environment than monomers without NADPH. Apart from packing, the sequence similarity between the two structures is ~ 80%.

NADPH-binding site

Observations of structures resolved in the presence of NADPH revealed that NADPH binds in the cleft on the surface of each subunit of the molecule formed between the α-helical and β-barrel regions [5]. In BLC, sixteen residues are involved in binding the NADPH molecule, among which Arg202 and His234 are strictly conserved compared to the residues Pro150, Ser200, Asp212, and His304 that are partly conserved in the NADPH binding pocket. The NADPH molecule was absent in all four monomers. This region shows a backbone root-mean-square deviation (rmsd) of 0.3Å between NADPH-bound and unbound structures. This value is similar to that of PMC-PR and human catalases with and without NADPH [6, 7]. Interestingly, most of the side-chain residues in the cleft showed a similar orientation between the monomers with and

without NADPH. Nicotinamide- and adenine-binding pockets in the cleft were filled by recruiting conserved water molecules in all the four subunits. Ser200 residue in the adenine-binding pocket involved in the recognition of the NADPH molecule [8] hydrogen-bonded to a conserved water molecule at an average distance of 3.5Å. The nicotinamide-binding pocket was occupied by two or three water molecules that form hydrogen bonds with the nicotinamide-moiety stabilizing residue His304, with an average distance of 2.9Å. Both the adenine- and nicotinamide- binding pockets recruited conserved water molecules in BLC and HEC without NADPH. The same result was observed when comparing the BMC-PR catalase structure (PDB ID: 1M85) solved at 2 Å resolution. Due to the lack of a Rossmann fold [32], Murthy et al (1981) proposed that the recognition of nucleotides by BLC was based on the surface-charged residues in the binding pocket. Mutations in the NADPH-binding pockets of *E.coli* to the BLC sequence did not promote the NADPH binding, suggesting that NADPH binding affinity does not depend mainly upon the charged residues, even though they are conserved in the binding pocket [33]. Accordingly, the underlying cause of higher binding affinity for NADPH by mammalian catalase is unknown.

NADPH-linked changes in the active site of wild type catalase

The cavities of the four active sites bury a heme molecule at 20Å from their surface. The heme group in each subunit makes three hydrogen bonds with residues Arg71, His361, and Arg111 residues; four hydrogen bonds with two water molecules were noted in all four monomers. A similar kind of heme environment was discerned in human catalase subunits with and without NADPH. The orientation and interaction of three arginine residues, Arg71, Arg111, and Arg365 that supposedly increase the redox potential of the heme during the formation of compound I [12] are similar. The heme iron coordinate with Tyr357 residue at an average distance of 1.8Å compared to 1.94Å in HEC. These results showed that presence and absence of NADPH do not alter significantly heme and its environment. This finding also was confirmed through EPR spectroscopy of BLC without and with NADPH [21]; the specific activity in the former case was 3.8μM compared to 3.9μM in the latter [21]. Each subunit of the wild type structure has a catalytic water molecule 49(A), 30(B), 993(C), 60(D) in close proximity to the heme moiety with an average Fe-W distance of 3.6Å comparable to 4.09Å observed in human catalase molecules [6]. Such distances suggest that there is no direct coordination between this water molecule and heme Fe (**Figure 2A**). These water molecules are stabilized by the formation of hydrogen bonds with His74 and Asn147 at an average distance of 2.93Å and 3.32Å, respectively.

Active site analysis of NADPH-depleted cyanide and azide structures

Although all the four catalytic active sites in the cyanide complex structure are exposed to the solvent, the inhibitor cyanide preferably binds to only two of the active sites. The remaining two sites lack the cyanide molecule and the catalytic water molecule. This differs from the structure of the human catalase-cyanide inhibitor complex wherein all the four active sites have cyanide molecules. These sites form a direct coordination with the Fe atom of heme at an average distance of 1.62Å with N-C-Fe angle 162° (**Figure 2B**). Such tilted orientation of cyanide with heme at an angle of 155° was observed in the structure of the cytochrome c cyanide complex [34], whereas, in human catalase, cyanide binds linearly to the heme with a Fe^{3+}-CN distance of 1.6 Å [6]. The cyanide N-atom is strongly hydrogen-bonded with the catalytic water molecule at an average distance of 2.53Å in both the subunits. However, the distance between His74 and the catalytic water molecule was greater, viz. 3.56Å. This exclusion by cyanide of the water molecule from His74 probably hindered the molecule's adoption of a linear orientation. Cyanide binding did not alter the proximal side Tyr357- to-Fe distance of 1.8Å. In the two subunits without catalytic water molecule/cyanide, the heme moiety is slightly saddle shaped rather than planar as in wild-type catalase.

In the presence of another non-specific inhibitor of catalase, azide at 3mM, only one catalytic site interacts with azide molecule, while one has a catalytic water molecule; the remaining two catalytic sites have neither one of them. The result was same when catalase was co-crystallized with 10mM azide. In contrast, the azide molecule binds to heme in all four catalytic sites in the SCC-A, even when only a trace

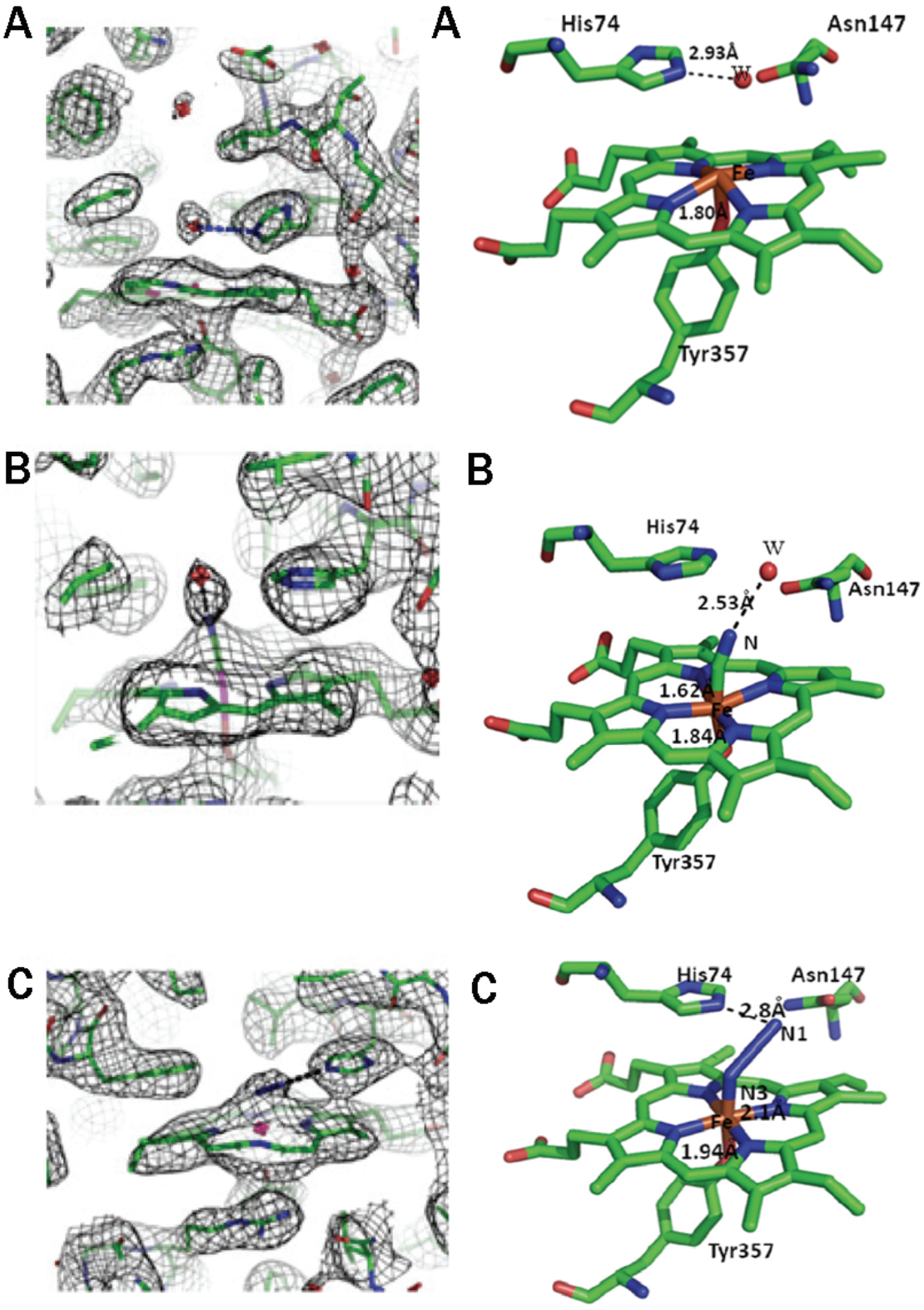

Figure 2. Active site composite omit maps (at 1σ cutoff) and ball & stick diagram of (A) wild- type catalase (1TGU), (B) wild-type catalase with cyanide (1TH3) and (C) wild-type catalase with azide (1TH2) are shown. The water molecules and iron atoms are represented as W and Fe respectively. The hydrogen bond interactions are shown in dotted lines.

(μM) amount of azide is present in the crystallization buffer [8]. In the wild-type catalase, azide inhibited the active site; the azide's electron density extended from the heme molecule to His74 (**Figure 2C**). The Fe-N distance was 2.1Å implying a direct coordination between azide and the heme molecule. The Fe- N1 (azide)-N2 (azide) angle is 116° compared 130° in the azide complex SCC-A [8]. This bending allows the interaction of the azide's N atom with His74, The distance between them being 2.8Å. This interaction eliminates the catalytic water molecule from the active site, and the bending ensures that it occupies the complete active site pocket. Such a tilt in the orientations of the azide molecule towards His74 also was evident observed in SCC-A catalase. The other subunit with catalytic water molecule interacted with His74 and Asn147 as in the wild-type catalase.

Discussion

We completely depleted NADPH from all the four monomers and made the complexes with cyanide and azide to study the role of NADPH in BLC. BLC has almost 80% sequence similarity with human catalase, as well as the same conserved active-site residues. In the human catalase tetramer, only two monomers have an NADPH molecule. Wild type crystallizes in $P2_12_12_1$ as does that of human catalase, and BLC with NADPH (4BLC). The presence or absence of NADPH does not significantly affect overall crystal packing, except that in HEC the packing environment differs between subunits with and without NADPH. So, it is worthwhile to discuss the details of human catalase structures and BLC with NADPH.

NADPH has fewer roles to play during the normal reaction cycle

During the normal reaction cycle, the enzyme shuttles between the ground state (Fe(III) state) and compound I state (oxy ferryl state), which involves the cleavage of two hydrogen-per-oxide molecules into two water molecules and an oxygen molecule [11-13]. It is established that the NADPH molecule has not direct role during the normal reaction cycle [19]. The formation of the compound I state requires the presence of a catalytic water molecule that is involved in the active-site cavity's water network [6, 35, 36]. Observations of the catalytic water molecule and its interaction with His74 and Asn147 in the wild type catalase and human catalase are the same. Spectral studies suggest that the heme molecule does not undergo any major conformational change, and maintains its active site environment even after removing NADPH from BLC [21]. The presence of the catalytic water molecule in all the four catalytic sites and its hydrogen bonding pattern with His74 and Asn147 in the wild-type structure, further structurally confirms that NADPH does not play a major role in maintaining the normal reaction cycle.

NADPH may have a role during inhibitor binding

The most significant observation in the structures of the cyanide and azide complexes is the absence of active site catalytic water molecules and the inhibitors in two subunits. In human catalases, cyanide- and catalytic water-molecules are obvious in all the four catalytic sites and only two NADPH molecules bind to the tetramer [6]. Interestingly, 3-amino-1, 2, 4-triazole (3AT) that is a specific inhibitor for catalase preferably binds to monomers lacking a bound NADPH molecule [6]. Nevertheless, 3AT does not interact with heme (as is the case for cyanide and azide); rather, it forms an adduct with the catalytic water molecule stabilizing residue His75 (His74 in BLC). However, the different crystal packing environments between monomers with and without NADPH in human catalase possibly influence this difference in 3AT binding. However, the packing does not impose any hurdle for the inhibitor in reaching the active site. Hence, we speculate that the NADPH binding with monomer may have some role during inhibitor binding.

NADPH binding may sense through domain swapping

One possible explanation for the absence of the inhibitor in two subunits of wild-type catalase could be the absence of the catalytic water molecules in them because a continuous water network in the cavity of an active site plays a major role in ensuring that the substrate reaches the active site [36]. So, the absence of catalytic water molecule in the two subunits of wild-type complex leads to the breakdown of this continuous water network, thereby restricting the diffusion of inhibitors to the active sites. This explanation, however, does not fit the 3AT inhibited HEC structure. In that, even the

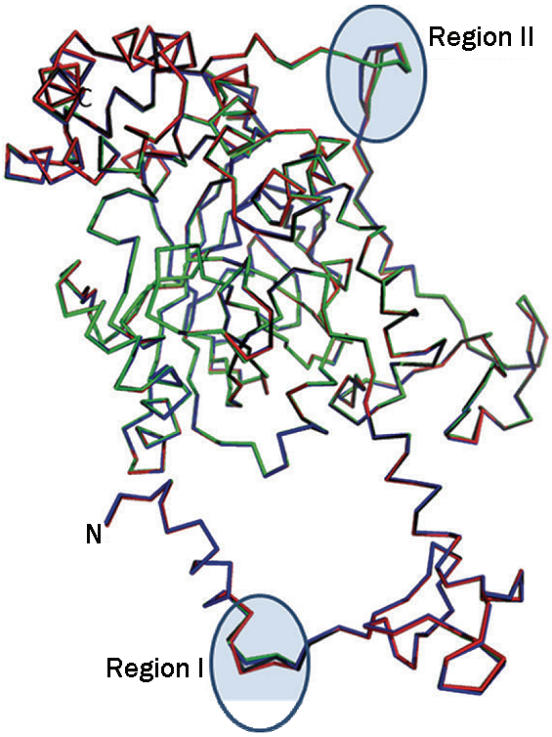

Figure 3. Cα superimposition of human catalase monomers with (blue and Green), and without NADPH (red and black). The N and C terminals are labeled. The circles showing the regions (I and II) have an rmsd of more than 1.5Å. Note that the region I is more distorted in monomers without NADPH.

monomers with a continuous water network in the active site's cavity lack the inhibitor 3AT. Hence, the explanation holds for the absence small sized inhibitors, like cyanide and azide, but not for 3AT.

Another explanation for the absence of inhibitors in two of the four subunits arises from the observation that the structures with an inhibitor or catalytic water molecule have an N-terminal domain-swapped linkage with subunits without an inhibitor. Superimposing a monomer of human catalase with and without NADPH revealed an rmsd more than 1Å in the hinge-loop region (residue 12-25: Region I), and also in the wrapping-loop region (residue 379-437: Region II) (**Figure 3**). This deviation is considerable since the structure is solved at 1.9Å resolution. Region I in the human catalase monomers with NADPH is highly ordered (rmsd of 0.35Å) compared to monomers without NADPH (rmsd of 1.6 Å). Region II has an rmsd more than 1Å, even for monomers with NADPH. This signifies that the deviation in region I is NADPH-dependent. The superimposition of BLC with and without NADPH also demonstrates an rmsd value of 1.5Å in the hinge-loop region (region I) and in the N-terminal helices. However, this value is not discernable at 2.8Å resolution. But the high accessible surface area (75Å^2) and thermal factor (>45Å^2) of the hinge-loop region confer high flexibility and make it structurally less stable. In addition to that the different packing environment of human catalase monomers with and without NADPH also influences deviation in the hinge loop. Thus, the calculated average value of helix distortion for N-terminal domain-swapped α-helix in HEC is, respectively, 6 and 11 for monomers with and without NADPH, compared with the ideal α-helix distortion value of 5. These values were calculated using the program developed by [37]. Our analyses show that the N-terminal domain-swapped helix is more distorted in human catalase monomers without NADPH than with NADPH. Mutation of the N-terminal α-helix stabilizing residue Gln10 in rat catalase (Gln11 in BLC and Gln12 in HEC) to His leads to an unstable enzyme [38]. This residue is conserved in all mammalian catalases and is involved in anchoring the N-terminal α-helix by interacting with R and Q-related subunits. In correspondence with the above studies, we suggest that the distorted N-terminal domain swapped α-helix in human catalase without NADPH might have some effect on the inhibitor's binding affinity of the catalytic pocket. In a broad sense, there is a possibility that the binding of NADPH in one subunit is communicated to the other domain-swapped subunit catalytic pocket either by stabilizing the N-terminal α-helix or by stabilizing both the N-terminal α-helix and the hinge-loop region (region I), thereby controlling the inhibitor binding. In support of such dimeric behavior, BLC purified as a dimer showed slightly higher enzyme activity than the native tetramer [39]. This involvement of 3D-domain swapping in allosteric signal transmission through ligand binding also is observed in membrane-associated guanylate kinases [40]. It is proposed that in domain- swapped proteins this kind of domain swapping structural elements sense ligand binding [41, 42] . Based on the above argument, we speculate that the domain-swapping elements the N-terminal hinge loop and the N-terminal α-helix act as putative sensors of NADPH binding.

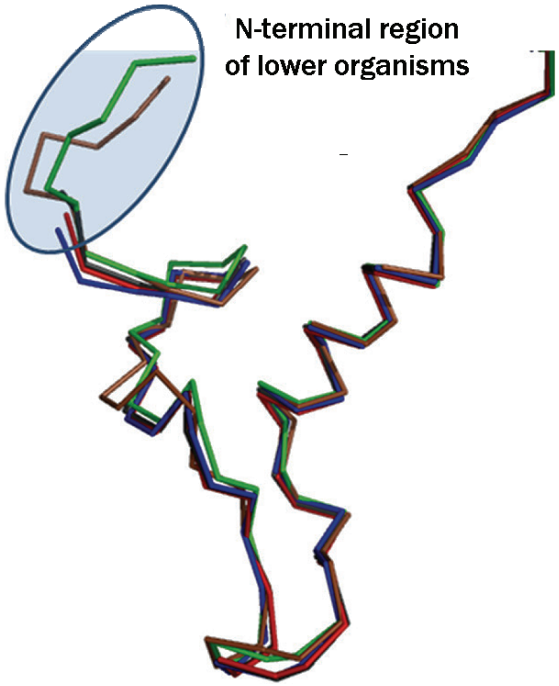

Figure 4. Cα superimposition of N-terminal domain swapped region of lower organism catalases PDB ID: 1M85 (Red), 1QWL (Green), 1SI8 (Blue), 1A4E (Brown) and 2ISA (Black). The encircled region represents the N-terminal region of fungal catalases. Note that the encircled region is a β-turn.

Putative NADPH binding sensors are not present in fungal catalases

The mammalian (BLC and human) and fungal catalases (SCC_A, PMC and MLC) have high sequence similarity in their active sites, heme binding, and catalytic residues. But mammalian catalases easily form the compound II state and are highly subject to inactivation induced by hydrogen peroxide, DTE and NH_2Cl compared to fungal catalases [20, 21, 43]. Mammalian catalase binds to NADPH with much higher affinity than the fungal catalases [10]. Adding NADPH to fungal catalase has a very minimal effect on the removal of the compound II state [20, 21]. The lower affinity of fungal catalases to NADPH (SCC-A and MLC) also is evident in their structures through the partial occupancy of NADPH [8, 9]. All the small subunit catalases superimpose with an average rmsd of 1.8Å. However, the N-terminal domain-swapped region of mammalian catalases have an α-helix (residues 10-17 in BLC), whereas it is a β-turn in almost all small subunit catalases from lower organisms (PDB ID: 1M85, 1QWL, 1SI8, 1A4E and 2ISA) (**Fiure 4**). There is no conserved residue or interaction in fungal catalases to stabilize the β-turn, as in the case of Gln in the N-terminal domain-swapped α-helix of mammalian catalases. Hence, the proposed allosteric signal transmission through ligand-binding signal transduction through domain swapping seemingly is likely only in mammalian catalases, not fungal catalases. Accordingly, we consider NADPH stabilization of the N-terminal domain-swapped α-helix plays a major function in mammalian catalase but not in fungal catalase. This maybe one reason why fungal catalases are less vulnerable to inactive state formation compared to mammalian catalases.

Although the above arguments we presented are speculative and need further verification, as a whole our studies have opened up a new possibility, viz. that mammalian catalase acts as a domain-swapped dimer of dimers, especially during inhibitor binding. To generalize this concept to the formation of the inactive state in mammalian catalases in the absence of tightly bound NADPH molecules needs further exploration. The present study adds one more intriguing fact to the existing mysteries of mammalian catalases.

Acknowledgements

We gratefully acknowledge Dr.Desigan Kumaran Ph.D, Prof.Subramanyam Swaminathan Ph.D, Biology Department, Brookhaven National Laboratory, Upton, New York 11973, USA for data collection at the beamline X29 (National Synchrotron Light Source) and structure determination. Preliminary BLC crystals studies were carried out using the X-ray facility for Structural Biology at the Molecular Biophysics Unit (MBU), Indian Institute of Science (IISc). The protein purification and computation facilities in Crystallography and Biophysics Department, Madras University (MU) are supported under the FIST program funded by the Department of Science and Technology, Government of India. Sugadev.R acknowledges the Council for Scientific and Industrial Research, Government of India, for a senior research fellowship. He also thanks Balasundaresan (MU) and Arockia Jeyaprakash (MBU) for helping him with X-ray studies and Prof.M R N Murthy (MBU) for useful discussions.

Please address correspondence to: Dr. Ragumani Sugadev, Bioinformatics Centre, Defense Institute of Physiology and Allied Science, Lucknow Road, Timarupr, Delhi-110054, India; Tel: 001-91-9718966994, 001-11-23883185, E-mail: ragusugadev@yahoo.com

References

[1] Kirkman H N and Gaetani GF. Mammalian catalase: a venerable enzyme with new mysteries. Trends Biochem Sci 2007;32:44-50.

[2] Melov S, Ravenscroft J, Malik S, Gill M S, Walker D W, Clayton PE, Wallace DC, Malfroy B, Doctrow SR and Lithgow GJ. Extension of lifespan with superoxide dismutase/catalase mimetics. Science 2000;289:1567-1569.

[3] Orr WC and Sohal RS. Extension of life-span by overexpression of superoxide dismutase and catalase in Drosophila melanogaster. Science 1994;263:1128-1130.

[4] Schriner SE, Linford NJ, Martin GM, Treuting P, Ogburn CE, Emond M, Coskun PE, Ladiges W, Wolf N, Van Remmen H, Wallace DC and Rabinovitch PS. Extension of murine life span by overexpression of catalase targeted to mitochondria. Science 2005;308:1909-1911.

[5] Murthy MR, Reid TJ, Sicignano A, Tanaka N and Rossmann MG. Structure of beef liver catalase. J Mol Biol 1981; 152:465-499.

[6] Putnam CD, Arvai AS, Bourne Y and Tainer JA. Active and inhibited human catalase structures: ligand and NADPH binding and catalytic mechanism. J Mol Biol 2000;296:295-309.

[7] Gouet P, Jouve HM and Dideberg O. Crystal structure of Proteus mirabilis PR catalase with and without bound NADPH. J Mol Biol 1995;249:933-954.

[8] Mate MJ, Zamocky M, Nykyri LM, Herzog C, Alzari PM, Betzel C, Koller F and Fita I. Structure of catalase-A from Saccharomyces cerevisiae. J Mol Biol 1999;286:135-149.

[9] Murshudov GN, Grebenko AI, Brannigan JA, Antson AA, Barynin VV, Dodson GG, Dauter Z, Wilson KS and Melik-Adamyan WR. The structures of Micrococcus lysodeikticus catalase, its ferryl intermediate (compound II) and NADPH complex. Acta Crystallogr D Biol Crystallogr 2002;58:1972-1982.

[10] Kirkman HN, Galiano S and Gaetani GF. The function of catalase-bound NADPH. J Biol Chem 1987;262:660-666.

[11] Deisseroth A and Dounce AL. Catalase: Physical and chemical properties, mechanism of catalysis, and physiological role. Physiol Rev 1970;50:319-375.

[12] von Ossowski I, Hausner G and Loewen PC. Molecular evolutionary analysis based on the amino acid sequence of catalase. J Mol Evol 1993;37:71-76.

[13] Ivancich A, Jouve HM, Sartor B and Gaillard J. EPR investigation of compound I in Proteus mirabilis and bovine liver catalases: formation of porphyrin and tyrosyl radical intermediates. Biochemistry 1997;36:9356-9364.

[14] Hillar A and Nicholls P. A mechanism for NADPH inhibition of catalase compound II formation. FEBS Lett 1992; 314: 179-182.

[15] Gebicka L, Metodiewa D and Gebicki JL. Pulse radiolysis of catalase in solution. I. Reactions of O2- with catalase and its compound I. Int J Radiat Biol 1989;55:45-50.

[16] Keilin D and Nicholls P. Reactions of catalase with hydrogen peroxide and hydrogen donors. Biochim Biophys Acta 1958:29, 302-307.

[17] Lardinois OM. Reactions of bovine liver catalase with superoxide radicals and hydrogen peroxide. Free Radic Res 1995;22:251-274.

[18] Chance B. Effect of pH upon the reaction kinetics of the enzyme-substrate compounds of catalase. J Biol Chem 1952;194:471-481.

[19] Kirkman HN, Rolfo M, Ferraris AM and Gaetani GF. Mechanisms of protection of catalase by NADPH. Kinetics and stoichiometry. J Biol Chem 1999;274:13908-13914.

[20] Mashino T and Fridovich I. NADPH mediates the inactivation of bovine liver catalase by monochloroamine. Arch Biochem Biophys 1988;265:279-285.

[21] Jouve HM, Pelmont J and Gaillard J. Interaction between pyridine adenine dinucleotides and bovine liver catalase: a chromatographic and spectral study. Arch Biochem Biophys 1986;248:71-79.

[22] Margoliash E, Novogrodsky A. and Schejter A. Irreversible reaction of 3-amino-1:2:4-triazole and related inhibitors with the protein of catalase. Biochem J 1960;74:339-348.

[23] Beers RF, Jr and Sizer IW. A spectrophotometric method for measuring the breakdown of hydrogen peroxide by catalase. J Biol Chem 1952;195:133-140.

[24] Arnao MB, Acosta M, del Rio JA and Garcia-Canovas F. Inactivation of peroxidase by hydrogen peroxide and its protection by a reductant agent. Biochim Biophys Acta 1990;1038:85-89.

[25] Otwinowski Z and Minor W. Methods in Enzymol 1997;276:307-326

[26] Navaza J. Implementation of molecular replacement in AMoRe. Acta Crystallogr D Biol Crystallogr 2001;57:1367-1372.

[27] Jones TA, Zou JY, Cowan SW and Kjeldgaard M. Improved methods for the building of protein models in electron density maps and the location of errors in these models. *Acta Crystallogr. Sect. A* 1991;A47:110-119.

[28] Brunger AT, Adams PD, Clore GM, DeLano WL, Gros P, Grosse-Kunstleve RW, Jiang J S, Kuszewski J, Nilges M, Pannu NS, Read RJ, Rice LM, Simonson T and Warren GL Crystallography & NMR system: A new software suite for macromolecular structure determination.

Acta Crystallogr D Biol Crystallogr 1998;54:905-921.
[29] Laskowski RA, MacArthur MW, Moss DS and Thornton JM. PRO-CHECK: a program to check the stereochemical quality of protein structures. *J. Appl. Crystallogr.* 1993;26:283-291.
[30] Hubbard SJ and Thornton JM. 'NACCESS', Computer Program. Department of Biochemistry and Molecular Biology, University College London, 1993.
[31] DeLano WL. PyMOL- a molecular graphics system. DeLano scientific, San Carlos, CA, USA, 1998.
[32] Rossmann MG, Moras D and Olsen KW. Chemical and biological evolution of nucleotide-binding protein. Nature 1974;250:194-199.
[33] Sevinc MS, Mate MJ, Switala J, Fita I and Loewen PC. Role of the lateral channel in catalase HPII of Escherichia coli. Protein Sci 1999;8:490-498.
[34] Leys D, Backers, K, Meyer TE, Hagen WR, Cusanovich MA and Van Beeumen JJ. Crystal structures of an oxygen-binding cytochrome c from Rhodobacter sphaeroides. J Biol Chem 2000;275:16050-16056.
[35] Fita I and Rossmann MG. The NADPH binding site on beef liver catalase. Proc Natl Acad Sci U S A 1985;82:1604-1608.
[36] Melik-Adamyan W, Bravo J, Carpena X, Switala J, Mate M J, Fita I and Loewen PC. Substrate flow in catalases deduced from the crystal structures of active site variants of HPII from Escherichia coli. Proteins 2001;44:270-281.
[37] Rajan SS and Srinivasan R. Helical segment analysis of alpha-helical regions in proteins. Biopolymers 1977;16: 1617-1634.
[38] Shaffer JB and Preston KE. Molecular analysis of an acatalasemic mouse mutant. Biochem Biophys Res Commun 1990;173:1043-1050.
[39] Prakash K, Prajapati S, Ahmad A, Jain SK. and Bhakuni V. Unique oligomeric intermediates of bovine liver catalase. Protein Sci 2002;11:46-57.
[40] McGee AW, Dakoji SR, Olsen O, Bredt DS, Lim WA. and Prehoda KE. Structure of the SH3-guanylate kinase module from PSD-95 suggests a mechanism for regulated assembly of MAGUK scaffolding proteins. Mol Cell 2001;8:1291-1301.
[41] Freire E. The propagation of binding interactions to remote sites in proteins: analysis of the binding of the monoclonal antibody D1.3 to lysozyme. Proc Natl Acad Sci U S A 1999;96:10118-10122.
[42] Freire E. Can allosteric regulation be predicted from structure? Proc Natl Acad Sci U S A 2000;97:11680-11682.
[43] Lardinois OM, Mestdagh MM and Rouxhet PG. Reversible inhibition and irreversible inactivation of catalase in presence of hydrogen peroxide. Biochim Biophys Acta 1996;1295:222-238.